



Original Article

Chuanxiong Rhizoma extracts prevent liver fibrosis via targeting CTCF-c-MYC-H19 pathway

Yajing Li ^a, Fanghong Li ^b, Mingning Ding ^a, Zhi Ma ^a, Shuo Li ^b, Jiaorong Qu ^a, Xiaojiaoyang Li ^{a,*}

^aSchool of Life Sciences, Beijing University of Chinese Medicine, Beijing 100029, China

^bSchool of Chinese Materia Medica, Beijing University of Chinese Medicine, Beijing 100029, China

ARTICLE INFO

Article history:

Received 1 March 2023

Revised 7 May 2023

Accepted 25 July 2023

Available online 28 November 2023

Keywords:

Chuanxiong Rhizoma

cholangiocytes

ductular reaction

Ligusticum chuanxiong Hort.

liver fibrosis

lncRNA H19

ABSTRACT

Objective: Hepatic fibrosis has been widely considered as a conjoint consequence of almost all chronic liver diseases. *Chuanxiong Rhizoma* (Chuanxiong in Chinese, CX) is a traditional Chinese herbal product to prevent cerebrovascular, gynecologic and hepatic diseases. Our previous study found that CX extracts significantly reduced collagen contraction force of hepatic stellate cells (HSCs). Here, this study aimed to compare the protection of different CX extracts on bile duct ligation (BDL)-induced liver fibrosis and investigate plausible underlying mechanisms.

Methods: The active compounds of CX extracts were identified by high performance liquid chromatography (HPLC). Network pharmacology was used to determine potential targets of CX against hepatic fibrosis. Bile duct hyperplasia and liver fibrosis were evaluated by serologic testing and histopathological evaluation. The expression of targets of interest was determined by quantitative real-time PCR (qPCR) and Western blot.

Results: Different CX extracts were identified by tetramethylpyrazine, ferulic acid and senkyunolide A. Based on the network pharmacological analysis, 42 overlap targets were obtained via merging the candidates targets of CX and liver fibrosis. Different aqueous, alkaloid and phthalide extracts of CX (CX_{AE}, CX_{AL} and CX_{PHL}) significantly inhibited diffuse severe bile duct hyperplasia and thus suppressed hepatic fibrosis by decreasing CCCTC binding factor (CTCF)-c-MYC-long non-coding RNA H19 (H19) pathway in the BDL-induced mouse model. Meanwhile, CX extracts, especially CX_{AL} and CX_{PHL} also suppressed CTCF-c-MYC-H19 pathway and inhibited ductular reaction in cholangiocytes stimulated with taurocholate acid (TCA), lithocholic acid (LCA) and transforming growth factor beta (TGF- β), as illustrated by decreased bile duct proliferation markers.

Conclusion: Our data supported that different CX extracts, especially CX_{AL} and CX_{PHL} significantly alleviated hepatic fibrosis and bile duct hyperplasia via inhibiting CTCF-c-MYC-H19 pathway, providing novel insights into the anti-fibrotic mechanism of CX.

© 2023 Tianjin Press of Chinese Herbal Medicines. Published by ELSEVIER B.V. This is an open access article under the CC BY-NC-ND license (<http://creativecommons.org/licenses/by-nc-nd/4.0/>).

1. Introduction

Liver fibrosis is a wound-healing response and is characterized by the deposition of extracellular matrix (ECM), which has been widely considered as a conjoint consequence of almost all chronic liver diseases (Zhang, Liu, Wang, & Sui, 2020). If left untreated, the continuum of fibrotic liver abnormalities will further progress to cirrhosis and even hepatocellular carcinoma (Parola & Pinzani, 2019). Among the pathogenic factors of liver fibrosis, the hepatic retention of bile acids (BAs) and excessive ductular reaction (DR) can lead to multiple strictures and obstructing of both intra- and

extra-hepatic bile ducts, which will develop into more aggressive hepatobiliary diseases clinically named as primary sclerosing cholangitis (PSC) and primary biliary cholangitis (PBC) (Aseem et al., 2021). In the bile duct ligation (BDL)-induced experimental model, cholangiocytes are sensitive to overloaded BAs or intracellular pathogenic molecules secreted by diverse hepatic cells and then proliferate significantly more rapidly to participate in the progression of liver fibrosis (Huang et al., 2016). While, ursodeoxycholic acid (UDCA), a capital FDA-approved pharmacotherapy for PBC or liver fibrosis complications, may stimulate several side effects including diarrhea and additional urticaria in the clinical application (Hirschfield et al., 2021). Thus, there is an unmet need to discover novel anti-fibrotic drugs targeting hyperproliferative or injured cholangiocytes.

* Corresponding author.

E-mail address: xiaojiaoyang.li@bucm.edu.cn (X. Li).

Increasing studies commit to clarify the underlying mechanisms of DR pathogenesis. *H19*, an imprinted and maternally expressed gene, is one of a few long noncoding RNAs (lncRNAs) conserved between human and mouse, playing a key role in the regulation of cell proliferation and differentiation (Li & Liu, 2020). We previously demonstrated that *H19* was dramatically upregulated in the cholangiocytes of carbon tetrachloride (CCl₄)-induced cirrhosis and BDL-induced fibrosis mouse models and was positively associated with disease progression (Li et al., 2017). Indeed, *H19* transcription can be regulated by several transcription factors and organizer of genome spatial. For instance, c-MYC bind to *H19* DNA sequence elements called E-boxes close to the imprinting control region (ICR) with its obligate heterodimerization partner Max, thus positively modulating *H19* transcription (Baryte-Lovejoy et al., 2006). CCCTC binding factor (CTCF), as another master organizer of genome spatial organization, regulates the imprinted genes *H19* by organizing chromatin at the *H19* locus (Freschi et al., 2021). Meanwhile, the transcriptional regulation of c-myc was mediated by a long-distance CTCF dependent enhancer-promoter interaction (Hyle et al., 2019). Notably, c-MYC and CTCF may also be involved in hepatic fibrosis by affecting phosphatidylinositol 3-kinase (PI3K)/AKT pathway (Liu et al., 2021; Salgado-Albarran, Spath, Gonzalez-Barríos, Baumbach, & Soto-Reyes, 2022). But until now, the regulation of c-MYC and CTCF in *H19*-related liver fibrosis is not well characterized and whether these targets could be prevented by any pharmacological therapies is unknown.

Traditional Chinese medicine (TCM), clinically used for thousands of years and generally considered to be safe, is a promising treatment against multiple chronic digestive diseases. *Chuanxiong Rhizoma* (Chuanxiong in Chinese, CX), the dried rhizome of *Ligusticum chuanxiong* Hort., has been demonstrated to prevent cerebrovascular, gynecologic and hepatic diseases via either using alone or in combination with other herbs (Rai et al., 2019; Wang et al., 2022; Wang et al., 2020). In clinical and experimental research, TCM formulas containing CX like Si-Wu-Tang and herb-pair of *Angelicae Sinensis Radix* and CX were reported to improve hepatitis and liver fibrosis via restoring multicellular function in multiple pathways (Ma et al., 2022; Wu et al., 2021). Furthermore, we previously found that tetramethylpyrazine (TMP), a representative bioactive ingredient derived from CX, ameliorated liver fibrosis via preventing the transfer of mitochondrial DNA from hepatocytes to hepatic stellate cells (HSCs) (Li et al., 2022). So far, hundreds of chemicals have been identified in CX and mainly belong to primary groups, including but not limited to alkaloids, phenolic acids and phthalides and the therapeutic promise of different extracts of CX has been emphasized (Huang et al., 2016). These studies encourage us to explore which extracts of CX play a major therapeutic role in relieving DR and whether the protection of CX against liver fibrosis are associated with the regulating of CTCF-c-MYC-*H19* pathway.

In this study, our data supported that different CX extracts, especially for alkaloid and phthalide extracts of CX (CX_{AL} and CX_{PHL}) alleviated hepatic fibrosis and cholangiocyte hyperproliferation via inhibiting CTCF-c-MYC-*H19* pathway both *in vivo* and *in vitro*, providing novel insights into the anti-fibrotic mechanism of CX.

2. Materials and methods

2.1. Materials

The traditional Chinese herb CX were purchased from Beijing Tongrentang (Group) Co., Ltd (China) and were performed by Dr. Bing Xu from the Beijing University of Chinese Medicine. Ferulic

acid (A33754) and TMP (A45751) were purchased from Innocem (Beijing, China). Senkyunolide A (PS2132) was purchased from Push Bio-Technology (Chengdu, China). Human TGF- β 1 (CA59) and lithocholic acid (LCA) (434-13-9) were purchased from Novoprotein Scientific Inc. (Shanghai, China). Chlorogenic acid (B20782) and taurocholic acid (TCA) (S30708) were purchased from Yuanye BioTechnology (Shanghai, China).

2.2. Separation and identification of different CX extracts

The four different extracts of CX including CX_{AE}, CX_{AL}, CX_{PA} and CX_{PHL} were prepared as followed: (1) CX_{AE}: CXs were sliced and soaked for 1 h. The mixture was extracted twice with eight volumes of distilled water using the condensation reflux method. The aqueous extract was concentrated with a rotary evaporator, filtered twice, and stored at -80 °C. (2) CX_{AL}: The CXs were crushed and extracted twice with 15 times the amount of 80% ethanol, refluxing for 2.5 h each time. (3) After weighting, CXs were extracted twice with the 15 times amount of 80% (volume percentage) ethanol through a reflux extraction device. (4) The smashed air-dried CX was fully soaked in 95% ethanol for more than 1 h, and extracted with 15-fold volume of 95% ethanol using diaculation method. The condition for high performance liquid chromatography (HPLC) was provided in the [Supplementary files](#).

Methanol was used as the reference substance solution, and the concentration of reference liquid including chlorogenic acid, ferulic acid, tetramethylpyrazine and senkyunolide A were 0.2 mg/mL. The compounds of CX were analyzed by HPLC and performed on a ACQUITY-HPLC-BEH-C₁₈ column (2.1 mm × 150 mm, 1.7 μ m). The mobile phase used were (A) a mixture of 0.1% formic acid aqueous solution and (B) acetonitrile. The gradient elution program of CX AEs was as follows: 0–0.5 min, 5% A; 0.5–8 min, 5%–45% A; 8–10 min, 45% A; 10–11 min, 45%–48% A; 11–16 min, 48%–50% A; 16–18.5 min, 50%–60% A; 18.5–20 min, 60%–75% A; 20–22 min, 75%–90% A; 22–23 min, 90%–5% A; 23–25 min, 5% A. The total speed was 0.2 mL/min and 2 μ L samples were injected each time. The detection wave was 295 nm. The mobile phase used for CX AIs were (A) a mixture of ddH₂O solution and (B) acetonitrile. The gradient elution program of CXAE was as follows: 0–10 min, 5%–20% B; 10–22.5 min, 20%–40% B; 22.5–37.5 min, 40% B; 37.5–42.5 min, 40%–70% B; 42.5–60 min, 70%–80% B; 60–70 min, 80%–100% B. The total speed was 0.3 mL/min, and 2 μ L samples were injected each time. The detection wave was 280 nm. As for CX_{PA} and CX_{PHL}, the mobile phase was (A) 1% formic acid aqueous solution and (B) acetonitrile. The gradient elution program was as follows 0–0.2 min (5% A), 0.2–7.5 min (5% A–80% A), 7.5–8.0 min (80% A–100% A), 8.5–9.0 min (100% A–5% A), 9.0–10.0 min (5% A). The total speed was 0.4 mL/min, and 2 μ L samples were injected each time. The detection wave was 320 nm at 35 °C. The content of Senkyunolide I and Senkyunolide A were detected at 280 nm, and the content of chlorogenic acid, ferulic acid, ferulic acid methyl ester and ligustilide Z were detected at 320 nm.

2.3. Animal studies

Male and female C57BL/6J mice (nine weeks old, 24–25 g) were purchased from SIBEIFU Biotechnology Co., Ltd. (Beijing, China). All mice were kept under 12 h light/ 12 h dark cycle at a consistent temperature (22 ± 2) °C and provided with standard chow with access to sterile water *ad libitum*. After one week of acclimation, mice were randomly divided into six groups (*n* = 8): sham group, BDL group, BDL + CX_{AE} group, BDL + CX_{AL} group, BDL + CX_{PA} group, and BDL + CX_{PHL} group. Our preliminary results indicated that 50 mg/kg was the most effective for CX_{AE} extracts against cholestasis. According to the extraction yield (CX_{AL}: 19.82%, CX_{PA}: 33.41% and CX_{PHL}: 36.89%), we prepared an administration dose of

10 mg/kg (CX_{AL}), 17 mg/kg (CX_{PA}) and 18 mg/kg (CX_{PHL}). Mice in sham and BDL groups were subjected to sham operation or BDL surgery for 7 d (Liu et al., 2019), which was a well-accepted thereby to construct liver fibrosis mice. Mice in the other four groups were pre-administrated with CX extracts for 2 d, then subjected to BDL surgery and administrated with CX extracts for another 4 d after 3 days of post-operation. After being sacrificed at corresponding times, mouse serum was collected and liver samples were harvested and stored in a –80 °C freezer. All animal studies and procedures were performed in accordance with the guidelines of the Institutional Animal Care and Use Committee of Beijing University of Chinese Medicine (BUCM-4-20200730023160).

2.4. Network pharmacology-based prediction of effects of CX on liver fibrosis

First, all natural ingredients of CX were obtained from TCM system pharmacology database and literatures (TCMSP, <https://tcm-spw.com/tcmssp.php>). Furthermore, we selected out the potential active compounds by oral bioavailability (OB) and drug-likeness (DL) (threshold values set to be: OB > 30% and DL > 0.18). Only components meeting the threshold value were considered as potential active ingredients. The most probable biological targets were obtained from Swiss Target Prediction (<https://swisstargetprediction.ch>) and further screened by searching Uniprot (<https://www.uniprot.org>) for human normalization. The targets related to 'liver fibrosis' were obtained from Online Mendelian Inheritance in Man database (OMIM, <https://omim.org>) and Gene Cards (<https://www.genecards.org>). Common targets were selected but other targets were removed. In this study, targets obtained from network pharmacology were introduced into String data (<https://string-db.org>) and Cytoscape software. In addition, we further analyzed the relationship between the selected targets by establishing a protein–protein interaction (PPI), performing Gene ontology (GO) and Kyoto encyclopedia of genes and genomes (KEGG) enrichment analysis.

2.5. Biochemical assays

Serum was collected from blood sample after animal sacrificed. Serum alanine aminotransferase (ALT), aspartate aminotransferase (AST), total bilirubin (T-BIL) and gamma-glutamyl transferase (γ -GT) were measured by ALT assay kit (C009-2-1), AST assay kit (C010-2-1), T-BIL assay kit (C019-1-1) and γ -GT assay kit (C017-2-1).

2.6. Histopathology staining

Mice were sacrificed and the livers were immobilized with 4% FPA and embedded in paraffin. Tissues were cut into 4.5- μ m sections and stained with hematoxylin and eosin (H&E) and Masson trichrome staining as previously described (Li, Li, Xue, Wang, & Li, 2022). After dewaxing and rehydration, tissue sections were stained with Van Gieson's Stain Kit (RS3930) and imaged with Aperio Versa (Leica, Wetzlar, Germany).

2.7. Cell culture of HIBECs

Human biliary epithelial cells (HIBECs) were obtained from ATCC and cultured with Minimum eagle's medium (MEM) containing 10% fetal bovine serum (FBS), penicillin G (100 U/mL) and streptomycin (100 μ g/mL) in an incubator with a humidified atmosphere of 5% CO₂ at 37 °C for further experiments.

2.8. Quantitative real-time PCR (qRT-PCR)

Total RNA in HIBECs and liver tissues in mice was extracted with Fast Pure Cell/ Tissue Total RNA isolation kit (RC101-01, Vazyme Biotech) and was reverse-transcribed with HiScript III RT SuperMix (R323-01, Vazyme Biotech). The mRNA levels of targeted genes were detected by AceQ Universal SYBR qPCR Master Mix (Q511-02, Vazyme Biotech) and normalized with *Hprt1* as previously described (Zeng, Yuan, Cai, Tang, & Gao, 2021).

2.9. Western blotting

Total proteins of livers and cell samples were extracted with RIPA buffer (Beyotime, China). After being resolved in 10% SDS-PAGE gel, equal proteins were transferred to the PVDF membrane, blocked 5% milk at room temperature for 1 h, and incubated in specific primary antibodies at 4 °C overnight. After rinsing with TBST for three times, different targeted proteins were incubated with corresponding secondary antibodies, and were further detected on a Bio-Rad Gel Doc XR + Imaging System (CA, USA) and analyzed by Quantity-One software.

2.10. Statistical analysis

All data are repeated at least three times and presented as mean \pm SEM. GraphPad Prism 8 (Graph-Pad, San Diego, CA) was used to perform a one-way ANOVA to compare differences in results between multiple groups. *P* values < 0.05 were considered as statistically significant.

3. Results

3.1. Chemical characterization of different extracts of CX

To describe chemical characterization of CX, we established HPLC methodology and identified a total of 10 constituents of aqueous of CX (CX_{AE}) (Fig. 1A and Table S1), and we selected four chemical markers, including TMP (the specific representative component of CX) (Fig. 1B), senkyunolide A (the most abundant ingredient of CX) (Fig. 1D), ferulic acid (FA, the quality control component of CX as described in *Chinese Pharmacopoeia*) (Fig. 1C) and chlorogenic acid (CA) (Fig. 1E). Based on the representative compounds identified in CX_{AE}, we subsequently prepared and characterized different CX extracts including alkaloid, phenolic acid and phthalide extracts of CX (CX_{AL}, CX_{PA} and CX_{PHL}). Subsequently, we prepared 'Standard Mixture' (SM) (different standards containing TMP, FA, senkyunolide A and CA) to characterize the different CX extracts (Fig. 1F). Based on this method, we confirmed the CX_{AL} by labeling TMP (Fig. 2A and 2B) and identified the CX_{PA} by FA (Fig. 2C and 2D). Meanwhile, the CX_{PHL} was identified by senkyunolide A in Fig. 2E and 2F. Above all, the preparation and identification of different CX extracts including CX_{AE}, CX_{AL}, CX_{PA} and CX_{PHL} laid the ground for further research both *in vivo* and *in vitro*.

3.2. Network pharmacology prediction of CX against liver fibrosis

In order to clarify the influence of CX on liver fibrosis, the network pharmacology-based prediction was performed. In this study, a total of 77 ingredients of CX were extracted from TCMSP and 12 candidate components satisfied the rules of OB > 30% and DL > 0.18. In addition, 2047 known targets associated with liver fibrosis were screened from DrugBank database and 183 targets were derived from OMIM database. After eliminating the redundancy, 1884 targets related to liver fibrosis were retained. We obtained 42 overlap targets by merging the candidates targets of

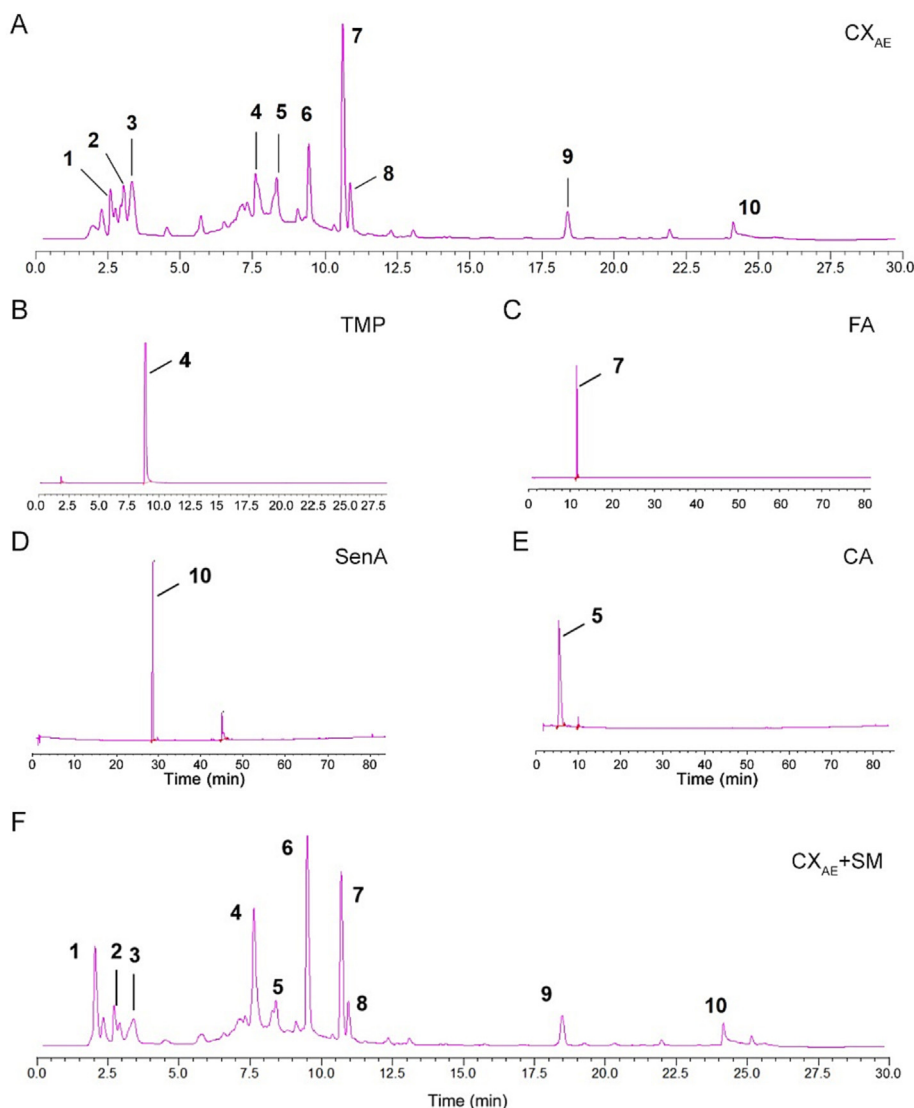


Fig. 1. HPLC spectrum profiles of representative extracts in CX_{AE} : HPLC spectrum profile of CX_{AE} (A), TMP (B), FA (C), SenA (D), CA (E) and $CX_{AE} + SM$ (F). CX_{AE} , aqueous extract of CX; TMP, tetramethylpyrazine; FA, ferulic acid; SenA, senkyunolide A; CA, citric acid; $CX_{AE} + SM$, aqueous extract of CX plus standard mixture.

CX and liver fibrosis (Fig. 3A). As shown in Fig. 3B, we calculated the main targets and established the potential connection between the targets. To scientifically unveil the underlying mechanism of CX on liver fibrosis, PPI network was obtained from Cytoscape software (Fig. 3C). Total 29 nodes and 128 edges were embodied in the network. Furthermore, in order to further clarified the categories of major hubs in the biological process (BP), molecular function (MF) and cellular components (CC), KEGG enrichment analysis was carried out on the major proteins, and the top 20 terms ($P < 0.05$) were selected as significant entries based on the P value (Fig. 3D). The KEGG categorical results indicated that majority of hubs were enriched in the BP, mainly including cellular response to inorganic substance, toxic substance and reactive oxygen species. Based on the KEGG enrichment analysis, we further established 'target-pathway' network to demonstrate the relationship between overlap targets and potential pathways through polychrome lines (Fig. 3E). Consistent with KEGG enrichment analysis results, the target proteins or genes involved in hyperproliferation and inflammatory response were identified, and among these targets, c-myc, CTCF, Cyclin D1 (CCND1), Cyclin D2 (CCND2), epithelial cell adhesion molecule (EPCAM), PI3K, Bcl2 and FOS were considered as the central link of the anti-fibrotic effects of CX, notably, most of which

were also related with the regulation of H19 or its-mediated function (Fig. 3F).

3.3. CX extracts ameliorate BDL-stimulated liver fibrosis in mice

To examine and compare the protection of CX extracts, we established BDL mouse model as described in 'Methods' (Fig. 4A) and observed that BDL significantly induced cholestatic liver fibrosis, as demonstrated by increasing serum ALT, AST, T-BIL and γ -GT, which were subsequently decreased by CX_{AE} , CX_{AL} and CX_{PHL} but not CX_{PA} (Supplementary Fig. S1 and Fig. 4B). As shown in Fig. 4C, liver histopathology study illustrated that CX_{AE} , CX_{AL} and CX_{PHL} reversed BDL-induced inflammation cell infiltration, diffuse severe bile duct hyperplasia, portal edema and mild portal infiltrates as demonstrated by HE and Masson's trichrome staining. Furthermore, collagen deposition was significant decreased in CX_{AE} , CX_{AL} and CX_{PHL} -treated groups by Van Gieson staining. In addition, the mRNA levels of liver fibrotic markers including *Fibronectin* and *Lox12* were markedly elevated by BDL and subsequently reversed by CX extracts including CX_{AE} , CX_{AL} and CX_{PHL} (Fig. 4D). During BDL-stimulated liver fibrosis, overloaded BAs stimulated cholangiocyte proliferation as illustrated by increasing mRNA

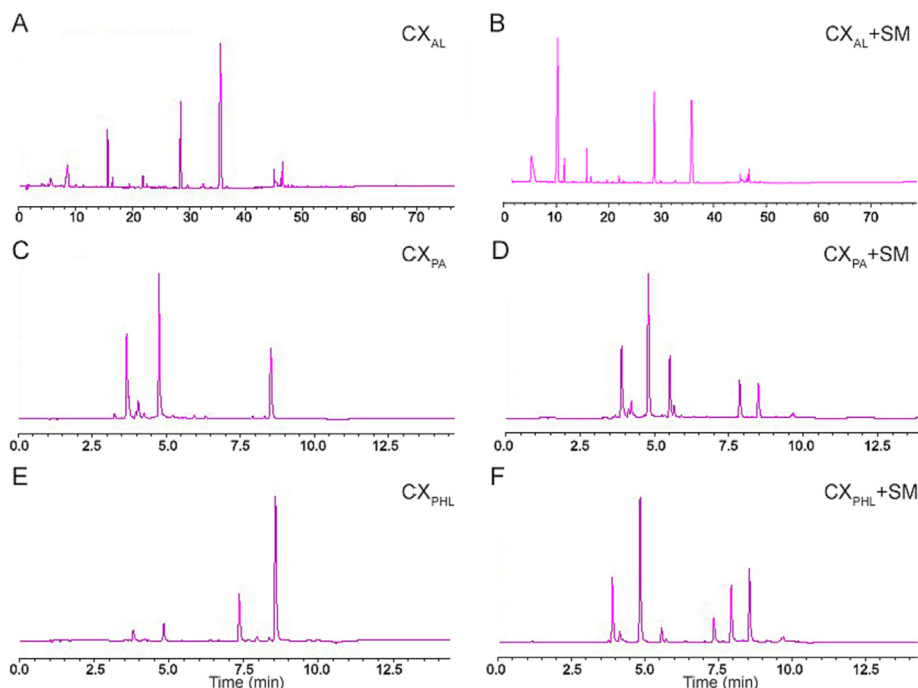


Fig. 2. Identified of three extracts in CX by HPLC. (A) HPLC spectrum profile of CX_{AL}. (B) HPLC spectrum profile of CX_{AL} + SM. (C) HPLC spectrum profile of CX_{PA}. (D) HPLC spectrum profile of CX_{PA} + SM. (E) HPLC spectrum profile of CX_{PHL}. (F) HPLC spectrum profile of CX_{PHL} + SM. CX_{AL}: alkaloid extract of CX; CX_{AE} + SM: alkaloid extract of CX plus standard mixture; CX_{PA}: phenolic acid extract of CX; CX_{PA} + SM: phenolic acid extract of CX plus standard mixture; CX_{PHL}: phthalide extracts of CX; CX_{PHL} + SM: phthalide extracts of CX plus standard mixture.

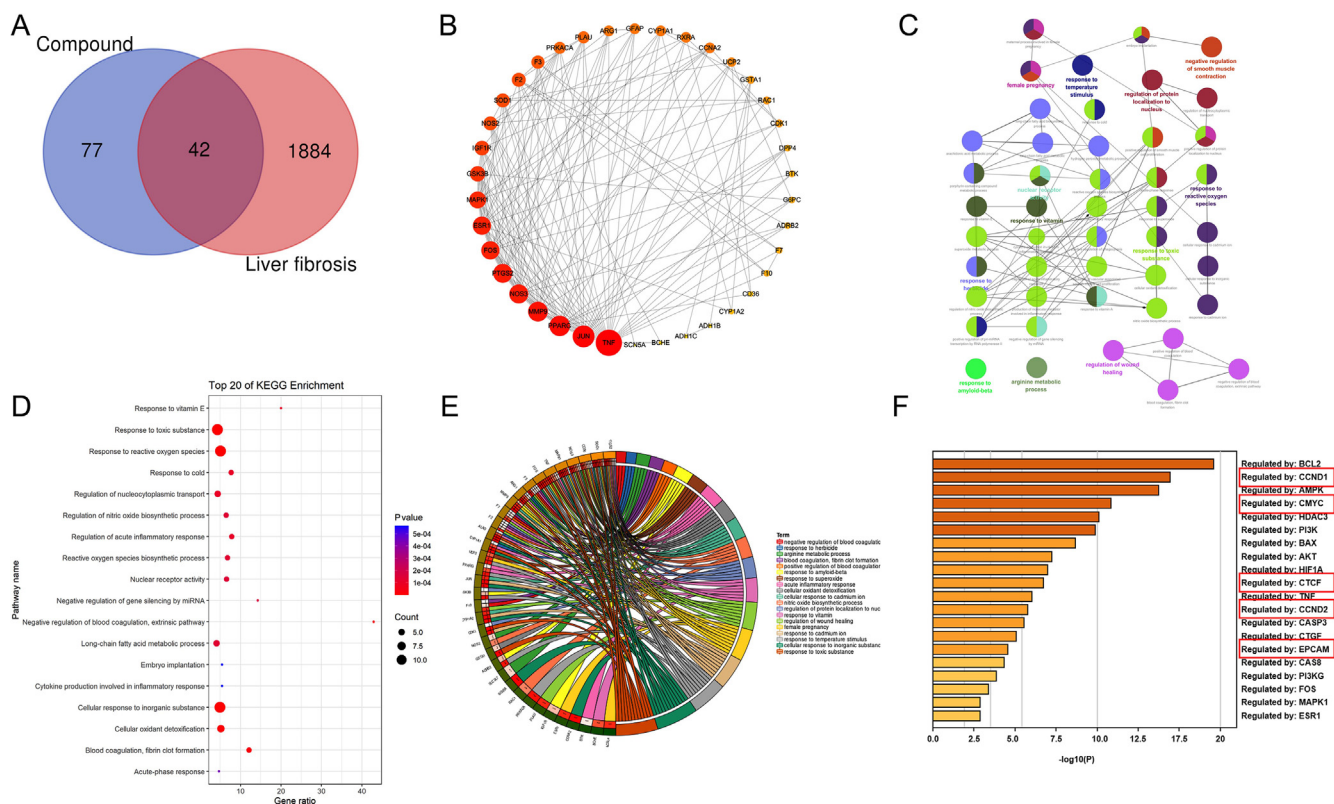


Fig. 3. Network pharmacological analysis. (A) Venn diagrams of potential targets of ‘CX’ and ‘liver fibrosis’. (B) Network of potential targets of CX and liver fibrosis analyzed by STING. The node size represented the connectivity degree, and thickness of the edges represented the combine score between targets. (C) PPI network. (D) KEGG analysis of potential targets of ‘CX’ and ‘liver fibrosis’. (E) ‘Targets-pathway’ network diagram. (F) ‘Potential Targets’ diagram.

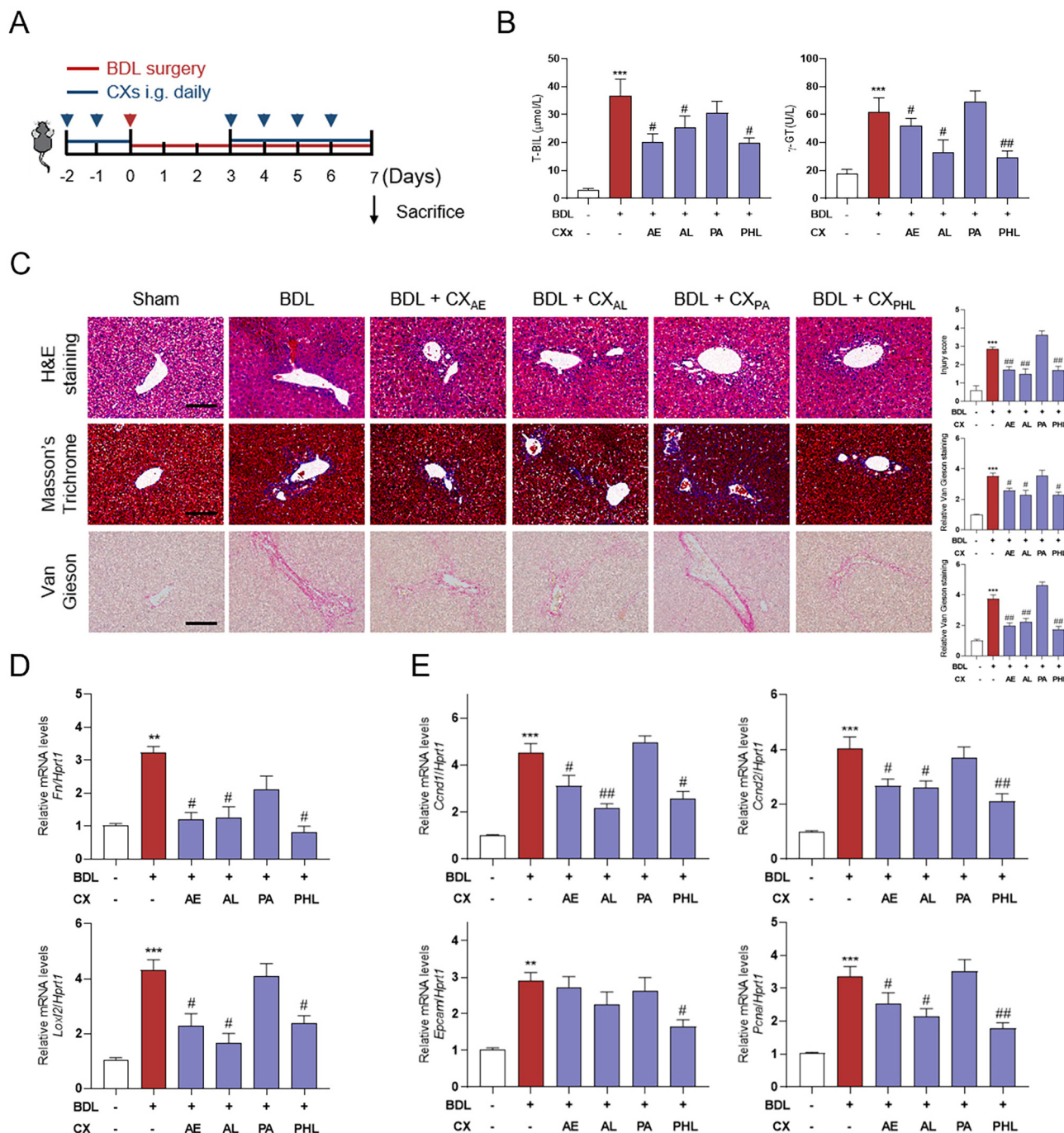


Fig. 4. CX extracts ameliorate BDL-stimulated bile duct hyperplasia and liver fibrosis (mean \pm SEM, $n = 6$). (A) Flowchart of animal experiments with associated photographic images of each group. (B) Serum T-BIL and γ -GT levels. (C) Representative images of H&E staining, Masson trichrome's staining and Van Gieson immunohistochemistry staining of liver tissues. And the quantified data were obtained using Image J software. Scale bar = 50 μm . Relative mRNA levels of (D) *Fn*, *Loxl2*, (E) *Cnd1*, *Cnd2*, *Epcam* and *Pcna* were determined by qPCR and normalized using *Hprt1* as an internal control. ^{*} $P < 0.01$, ^{***} $P < 0.001$, vs sham group; [#] $P < 0.05$, ^{##} $P < 0.01$ vs BDL group ($n = 8$).

levels of *Cnd1*, *Cnd2*, *Epcam* and proliferating cell nuclear antigen (*Pcna*). While, *CX_{AE}*, *CX_{AL}* and *CX_{PHL}* decreased the expression of these genes (but only *CX_{PHL}* decreased *Epcam* expression) and thus ameliorated cholangiocyte proliferation in liver fibrosis (Fig. 4E).

3.4. CX extracts alleviated bile duct hyperplasia via suppressing CTCF-c-MYC-H19 pathway

Given the anti-fibrotic effects of CX extracts *in vivo* and network pharmacology prediction, we next explored whether the underlying

mechanism of these protection was related with H19 and its related targets, c-myc and CTCF. Recently, we observed that herb pair containing CX significantly down-regulated the expression of H19, a hepatic fibrosis marker (J. Z. Wu et al., 2021) and similar suppressive effects on H19 were also found in different CX extracts (Fig. 5A). c-MYC promoted the transcription of the H19 via specifically binding directly to E-boxes close to the ICR. Meanwhile, CTCF sites at mammalian c-myc promoter and H19 imprinting control region, can regulate the transcription of H19 and c-myc (Liu et al., 2014; Ottema et al., 2021). Therefore, we detected the

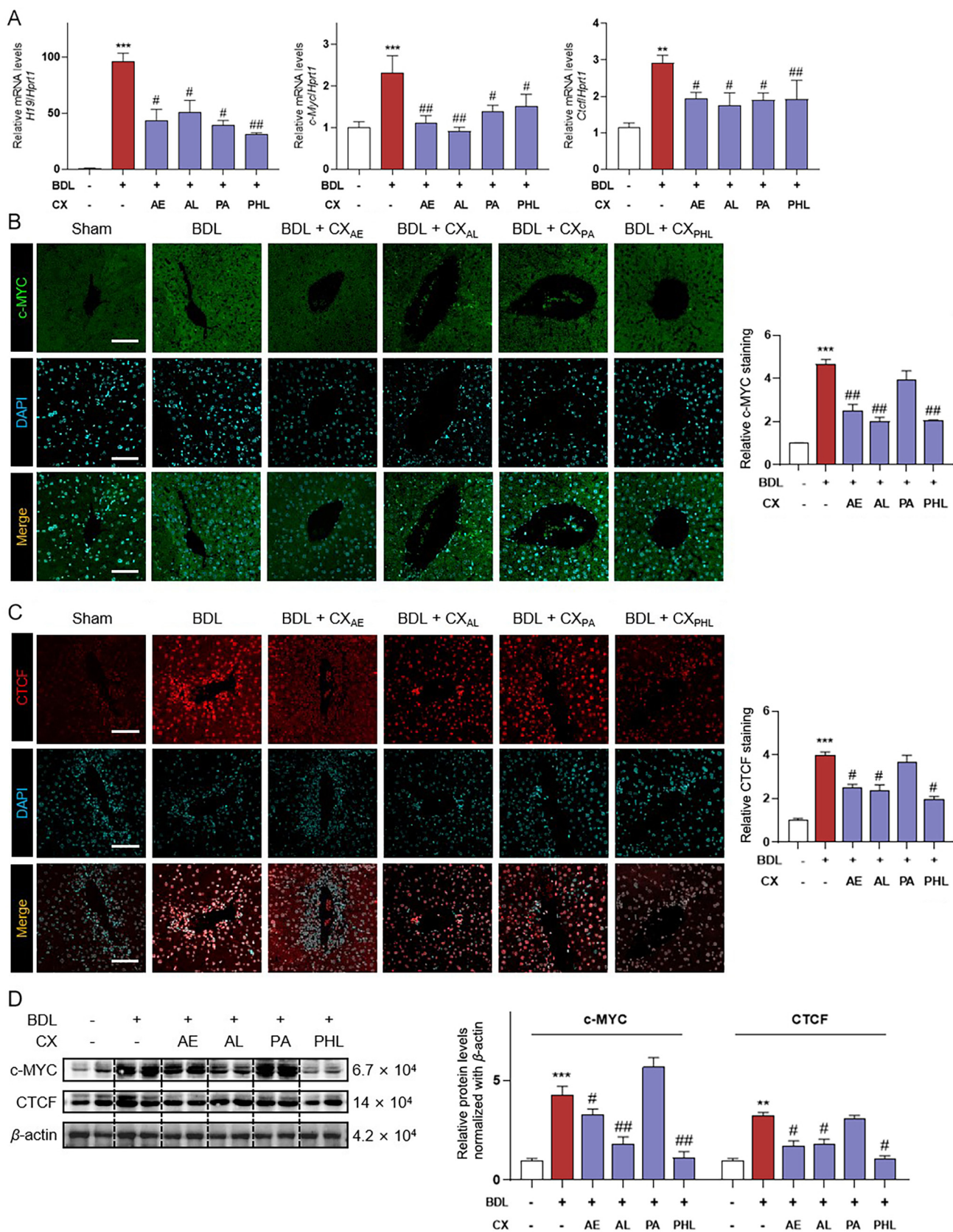


Fig. 5. CX extracts inhibit CTCF-c-MYC-H19 pathway in BDL-induced mice (mean ± SEM, n = 6). (A) Relative mRNA levels of *H19*, *c-myc* and *Ctf* determined by qPCR and normalized using *Hprt1* as an internal control. Representative images of c-MYC (B) and CTCF (C) staining of liver tissues. And the quantified data were obtained using Image J software. Scale bar = 50 μm. (D) Representative immunoblots against c-MYC, CTCF and β-actin in liver. **P < 0.01, ***P < 0.001 vs sham group; #P < 0.05, ##P < 0.01 vs BDL group (n = 8).

expression of *c-Myc* and *Ctcf* in different groups and found that CX_{AE}, CX_{AL}, CX_{PA} and CX_{PHL} significantly decreased the mRNA expression of *c-Myc* and *Ctcf* induced by BDL (Fig. 5A). Consistently, immunofluorescence staining indicated that BDL significantly increased the expression of c-MYC, which was subsequently down-regulated by CX_{AE} and CX_{PHL} (Fig. 5B). Similarly, CX_{AE} and CX_{PHL} markedly down-regulated the expression and distribution of CTCF, as illustrated by immunofluorescence staining in Fig. 5C. Furthermore, the protein levels of c-MYC and CTCF were also significantly elevated by BDL and subsequently reversed by some CX extracts, especially for CX_{AL} and CX_{PHL} (Fig. 5D). Collectively, these results demonstrated that CX extracts, especially CX_{AL} and CX_{PHL} alleviated cholangiocyte proliferation via suppressing CTCF-c-MYC-H19 pathway.

3.5. CX extracts especially CX_{PHL} alleviate overloaded BAs-related DR in cholangiocytes via suppressing CTCF-c-MYC-H19 pathway

Under the stimulus of BAs, cholangiocyte injury may be an early event in BDL-induced hepatic fibrosis due to their specific physiological position (Chen et al., 2021). Among the toxic BAs, TCA and LCA are major components and have been used to mimic BDL-induced excessive BAs *in vitro*. Meanwhile, TGF- β is responsive increased and lead to cholangiocytes proliferation and HSC activation in BDL mice (Wu et al., 2021). As shown in Fig. 6A–C, it was demonstrated that TCA, LCA and TGF- β significantly promoted cholangiocyte proliferation *in vitro* by increasing mRNA levels of different DR markers (*Epcam*, *Pcna* and *Cnd2*), which was reversed by CX_{AE}, CX_{AL} and CX_{PHL}. Meanwhile, immunofluorescence staining of CK-19 indicated that CX extracts especially CX_{AE}, CX_{AL} and CX_{PHL} significantly down-regulated TCA-, LCA- and TGF- β -stimulated DR in cholangiocytes (as shown by lower cytoplasmic expression) (Fig. 6D and Supplementary Fig. S2). Exactly, we have already confirmed that CX extracts suppressed bile duct hyperplasia in mice by targeting CTCF-c-MYC-H19 pathway (Fig. 5). Therefore, we subsequently detected the expression of the CTCF-c-MYC-H19 signaling in cholangiocytes and observed that CX_{AE}, CX_{AL} and CX_{PHL} markedly decreased the mRNA expression of *H19* and *c-myc* but gently down-regulated the *Ctcf* expression *in vitro* Fig. 7A–C. Consistently, as shown in Fig. 7D–F, the protein expression of CTCF and c-MYC were increased by TCA, LCA and TGF- β , which was subsequently down-regulated by CX_{AE}, CX_{AL} and CX_{PHL}. Notably, CX_{PHL} effectively decreased the expression of CTCF and c-MYC regardless of the stimulus, while CX_{AL} may be more sensitive to stimulation of TCA and TGF- β . Overall, CX extracts especially CX_{AL} and CX_{PHL} alleviate overloaded BAs-related DR in cholangiocytes via suppressing CTCF-c-MYC-H19 pathway. Overall, different CX extracts, especially for CX_{AL} and CX_{PHL} inhibited cholangiocyte hyperproliferation and liver fibrosis (Fig. 8).

4. Discussion

Liver fibrosis represents a dynamic wound healing process and the hepatoprotection of CX in ameliorating fibrotic liver disorders have been demonstrated in clinical trials and basic research (J. Wang et al., 2022). In the current study, different CX extracts were isolated and the representative components of these extracts were identified through 'Standard Mixture' (Figs. 1 and 2) then compared and investigated the anti-fibrotic effects of different CX extracts at the equivalent dose in liver fibrosis both *in vitro* and *in vivo* (Figs. 3–7). We found that CX_{AE}, CX_{AL} and CX_{PHL} concurrently alleviated liver fibrosis to varying degrees, as illustrated by the suppression of serum T-BIL and γ -GGT, hepatocytes vacuolation, ECM accumulation. Interestingly, among these CX extracts, more obvious anti-fibrotic activity of CX_{AL} and CX_{PHL} has been

observed, as demonstrated by the more significant inhibition of the levels of proliferation and DR markers both *in vitro* and *in vivo*. While, compared with CX_{AL}, CX_{PHL} may be the main contributor to the anti-fibrotic effects of CX, as illustrated by more obvious suppressive effects on the CTCF-c-MYC-H19 pathway. These events suggested that the hepatoprotective components in CX may be primarily derived from CX_{AL} and CX_{PHL}.

Indeed, researchers gradually pay attention to clarify the active compounds of the protection of different CX extracts. Network pharmacology, integrating system biology, pharmacology and computer analysis technology, has been used in the exploration of the complicated relationships among components, targets and diseases (Dai et al., 2020). Notably, more and more researchers have applied network pharmacology to predict the active components and potential targets of TCM and explore its effects and mechanisms against different diseases (Liu et al., 2022). Recently, network pharmacology has been used to explore the hepatoprotective of TCM, such as the molecular mechanism of *Schisandra chinensis* (Turcz.) Baill. against liver injury, the therapeutic mechanism of Danggui-Chuanxiong herb-pair on liver fibrosis (Wu et al., 2021). In the present study, based on the network pharmacology analysis, we focused on the cholangiocyte proliferation and CTCF-c-MYC-H19 relative signaling pathway, which has been overlooked for a long time. According to experimental analysis, we found that the differential protection of CX extracts may be attributed to different components and their regulation of different pathways. For example, representative components of CX_{AL} and CX_{PHL}, including TMP (Li et al., 2022; Wang, Xu, Yang, Chen, & Zhang, 2015), ligustilide (Yang & Xing, 2021), ligustichuane A (Wan et al., 2022) and ligustichuane B (Qin et al., 2022) have been demonstrated to respectively affect c-myc or H19, which may explain the phenomenon about the superimposed regulation of these two CX extracts on CTCF-c-MYC-H19 pathway. While the components in CX_{PA} may suppress hepatic fibrosis via other pathways but not CTCF-c-MYC-H19. Overall, these events may lead to the differential protections of CX extracts in fibrotic liver injury.

Another interesting finding was that although both CX_{AL} and CX_{PHL} significantly suppressed liver fibrosis by targeting CTCF-c-MYC-H19 and DR, their regulation of individual targets is differential. Among these extracts, CX_{PHL} significantly decreased the expression of H19, c-myc and CTCF, while other extracts may mainly affect c-myc, but not CTCF (Figs. 5 and 7). H19 is predominantly expressed in cholangiocytes and play key roles in cholestatic liver injury that also has gradually become a recognized biomarker of liver fibrosis (Li et al., 2017). C-myc, a master transcriptional factor, regulates approximately 10%–15% of genes in the genome, and more importantly, playing critical roles in promoting H19 transcription by binding to the E-boxes in H19 DNA sequence (Wu et al., 2020). In addition, CTCF concurrently modulated the transcription of c-myc and H19, while CX extracts gently decreased the expression of CTCF. These events suggested that the regulation of CTCF on H19 transcription exist "two-pronged" effects. Therefore, we suspected that the more obvious anti-fibrotic effects of CX_{PHL} may be attributed to the dual suppression of c-MYC and CTCF and subsequent inhibition of H19-related cholangiocyte proliferation. Exactly, as a recognized inhibitor of c-MYC, 10058-F4 has been devoted to the clinical therapeutics and basic research of hepatocellular carcinoma (Luo et al., 2021; Wu et al., 2020). While, the inhibitor of CTCF have not yet been not fully recognized, only a handful inhibitor is still in the preclinical, such as ZL 201910562893.1. These results also suggested that development of effective strategies targeting c-MYC or synergistic effects of Chinese medicine and specific target inhibitors will have great therapeutic significance for liver fibrosis and its complications.

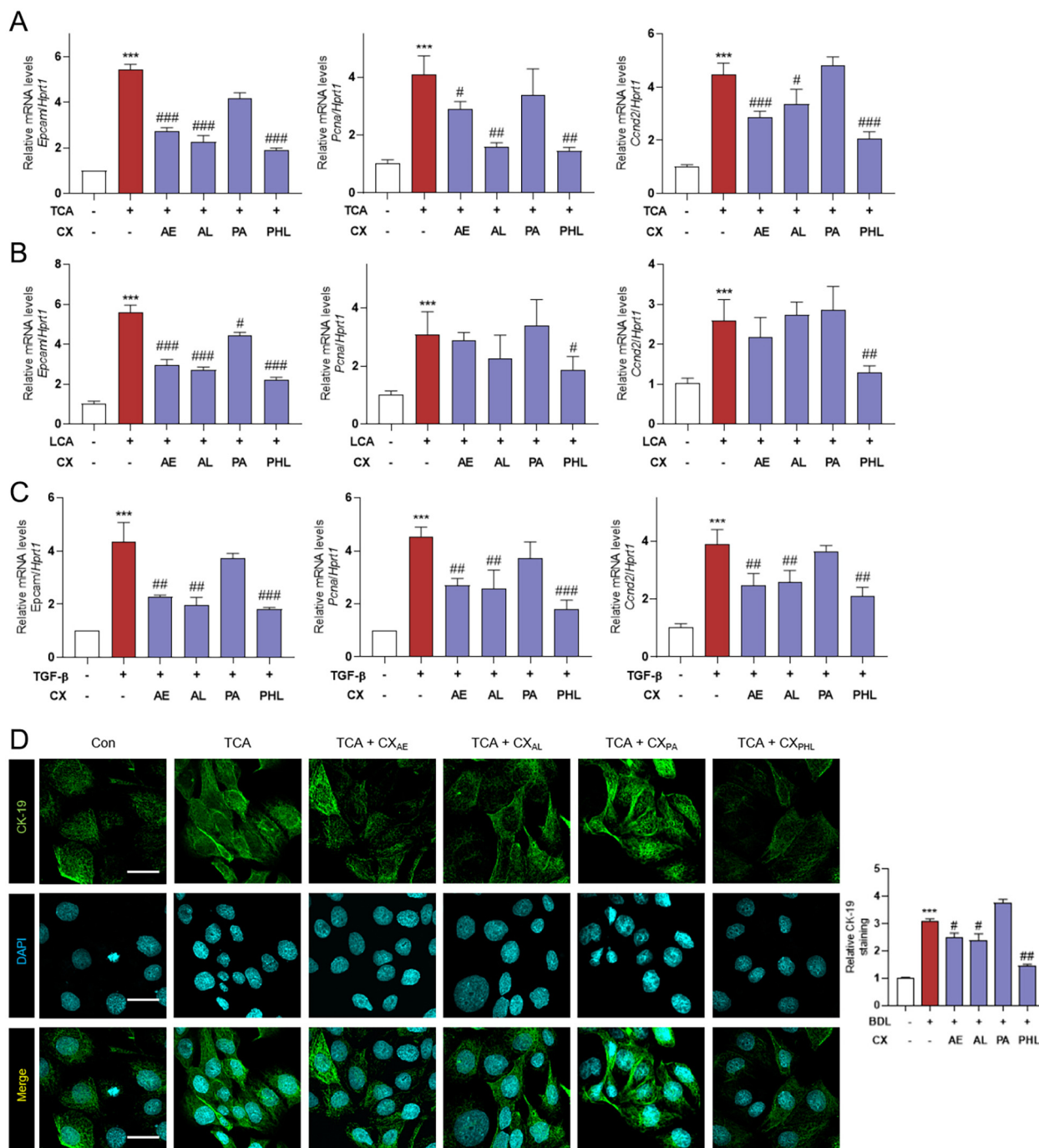


Fig. 6. CX extracts alleviate DR in TCA-, LCA- and TGF-β-induced cholangiocytes. Relative mRNA levels of *Epcam*, *Pcnal* and *Cnd2* were determined by qPCR and normalized using *Hprt1* as an internal control in (A) TCA-, (B) LCA- and (C) TGF-β-treated HIBECs (mean ± SEM, n = 3). (D) Representative images of immunofluorescent staining of CK-19 in TCA-treated HIBECs. And the quantified data were obtained using Image J software. Scale bar = 50 μm. Statistical significance: ***P < 0.001 vs sham group; #P < 0.05, ##P < 0.01, ###P < 0.001 vs BDL group.

5. Conclusion

Taken together, our results systemically indicated that different CX extracts significantly ameliorated liver fibrosis by disturbing CTCF-c-MYC-H19 pathway and alkaloid and phthalides from CX were the most effective fractions. Overall, these data offered a novel therapeutic strategy for DR-associated liver fibrosis and contribute to the discovery of CX-associated therapeutic agents for hepatic fibrosis.

CRediT authorship contribution statement

XL conceived the original idea and supervised the study. YL prepared the manuscript and figures. YL, FL, MD, ZM, SL and JQ conducted all the experiments and performed data analysis. All data were generated in-house and no paper mill was used. All authors have approved the final manuscript.

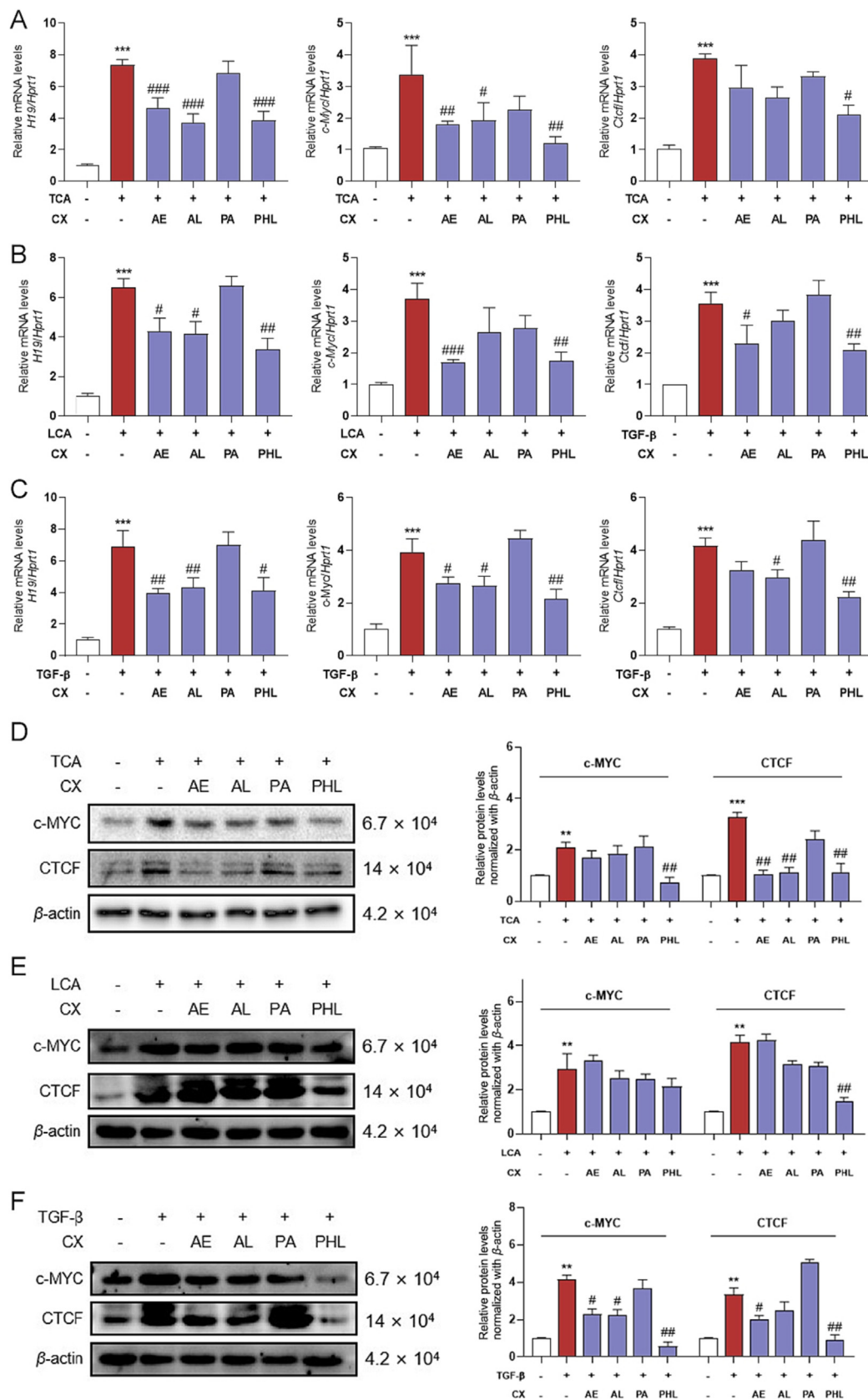


Fig. 7. CX extracts suppress CTCF-c-MYC-H19 pathway in cholangiocytes (mean ± SEM, n = 3). Relative mRNA levels of *H19*, *c-Myc* and *Ctcf* were determined by qPCR and normalized using *Hprt1* as an internal control in (A) TCA-, (B) LCA- and (C) TGF-β-treated HIBECs. Representative immunoblots against c-MYC, CTCF and β-actin in (D) TCA-, (E) LCA- and (F) TGF-β-treated HIBECs. Statistical significance: **P < 0.01, ***P < 0.001 vs sham group; #P < 0.05, ##P < 0.01, ###P < 0.001 vs BDL group.

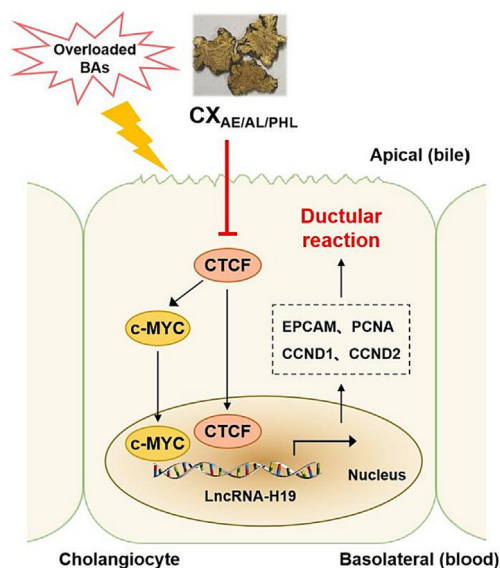


Fig. 8. Schematic diagram of proposed mechanisms of anti-fibrotic effects of CX extracts.

Declaration of Competing Interest

The authors declare that they have no known competing financial interests or personal relationships that could have appeared to influence the work reported in this paper.

Acknowledgements

This work was supported by the Beijing Municipal Science & Technology Commission (No. 7212174); the National High-Level Talents Special Support Program to XL; National Key Research and Development Program on Modernization of Traditional Chinese Medicine (No. 2022YFC3502100); National Natural Science Foundation of China (No. 82004045 and No. 82274186).

Appendix A. Supplementary data

Supplementary data to this article can be found online at <https://doi.org/10.1016/j.chmed.2023.07.003>.

References

- Aseem, S. O., Jalan-Sakrkar, N., Chi, C., Navarro-Corcuera, A., De Assuncao, T. M., Hamdan, F. H., ... Huebert, R. C. (2021). Epigenomic evaluation of cholangiocyte transforming growth factor-beta signaling identifies a selective role for histone 3 lysine 9 acetylation in biliary fibrosis. *Gastroenterology*, 160(3), 889–905 e810.
- Barsyte-Lovejoy, D., Lau, S. K., Boutros, P. C., Khosravi, F., Jurisica, I., Andrulis, I. L., ... Penn, L. Z. (2006). The c-Myc oncogene directly induces the H19 noncoding RNA by allele-specific binding to potentiate tumorigenesis. *Cancer Research*, 66(10), 5330–5337.
- Chen, L., Zhou, T., White, T., O'Brien, A., Chakraborty, S., Liangpunsakul, S., ... Glaser, S. (2021). The apelin-apelin receptor axis triggers cholangiocyte proliferation and liver fibrosis during mouse models of cholestasis. *Hepatology*, 73(6), 2411–2428.
- Dai, W., Tang, T., Dai, Z., Shi, D., Mo, L., & Zhang, Y. (2020). Probing the mechanism of hepatotoxicity of hexabromocyclododecanes through toxicological network analysis. *Environmental Science & Technology*, 54(23), 15235–15245.
- Freschi, A., Del Prete, R., Pignata, L., Cecere, F., Manfredola, F., Mattia, M., ... Cerrato, F. (2021). The number of the CTCF binding sites of the H19/IGF2:IG-DMR correlates with DNA methylation and expression imprinting in a humanized mouse model. *Human Molecular Genetics*, 30(16), 1509–1520.
- Hirschfield, G. M., Beuers, U., Kupcinskas, L., Ott, P., Bergquist, A., Farkkila, M., ... Poupon, R. (2021). A placebo-controlled randomised trial of budesonide for PBC following an insufficient response to UDCA. *Journal of Hepatology*, 74(2), 321–329.

- Huang, Y., Zhou, M., Li, C., Chen, Y., Fang, W., Xu, G., & Shi, X. (2016). Picroside II protects against sepsis via suppressing inflammation in mice. *American Journal of Translational Research*, 8(12), 5519–5531.
- Hyle, J., Zhang, Y., Wright, S., Xu, B., Shao, Y., Easton, J., ... Li, C. (2019). Acute depletion of CTCF directly affects MYC regulation through loss of enhancer-promoter looping. *Nucleic Acids Research*, 47(13), 6699–6713.
- Li, X., & Liu, R. (2020). Long non-coding RNA H19 in the liver-gut axis: A diagnostic marker and therapeutic target for liver diseases. *Experimental and Molecular Pathology*, 115, 104472.
- Li, X., Liu, R., Yang, J., Sun, L., Zhang, L., Jiang, Z., ... Zhou, H. (2017). The role of long noncoding RNA H19 in gender disparity of cholestatic liver injury in multidrug resistance 2 gene knockout mice. *Hepatology*, 66(3), 869–884.
- Li, Y., Li, S., Xue, X., Wang, T., & Li, X. (2022). Integrating systematic pharmacology-based strategy and experimental validation to explore mechanism of tripterygium glycoside on cholangiocyte-related liver injury. *Chinese Herbal Medicines*, 14(4), 563–575.
- Li, Y. J., Liu, R. P., Ding, M. N., Zheng, Q., Wu, J. Z., Xue, X. Y., ... Li, X. (2022). Tetramethylpyrazine prevents liver fibrotic injury in mice by targeting hepatocyte-derived and mitochondrial DNA-enriched extracellular vesicles. *Acta Pharmacologica Sinica*, 43(8), 2026–2041.
- Liu, Q., Yang, B., Xie, X., Wei, L., Liu, W., Yang, W., ... Qin, Y. (2014). Vigilin interacts with CCTC-binding factor (CTCF) and is involved in CTCF-dependent regulation of the imprinted genes Igf2 and H19. *The FEBS Journal*, 281(12), 2713–2725.
- Liu, R., Li, X., Zhu, W., Wang, Y., Zhao, D., Wang, X., ... Zhou, H. (2019). Cholangiocyte-derived exosomal long noncoding RNA H19 promotes hepatic stellate cell activation and cholestatic liver fibrosis. *Hepatology*, 70(4), 1317–1335.
- Liu, S., Yang, Q., Dong, B., Qi, C., Yang, T., Li, M., ... Wu, J. (2021). Gypenosides attenuate pulmonary fibrosis by inhibiting the AKT/mTOR/c-Myc pathway. *Frontiers in Pharmacology*, 12, 806312.
- Liu, S., Zhao, F., Deng, Y., Zeng, Y., Yan, B., Guo, J., & Gao, Q. (2022). Investigating the multi-target therapeutic mechanism of Gui Huang formula on chronic prostatitis. *Journal of Ethnopharmacology*, 294, 115386.
- Luo, Y., Yang, S., Wu, X., Takahashi, S., Sun, L., Cai, J., ... Gonzalez, F. J. (2021). Intestinal MYC modulates obesity-related metabolic dysfunction. *Nature Metabolism*, 3(7), 923–939.
- Ma, Z., Xue, X., Bai, J., Cai, Y., Jin, X., Jia, K., ... Li, X. (2022). Si Wu tang ameliorates bile duct ligation-induced liver fibrosis via modulating immune environment. *Biomedicine & Pharmacotherapy*, 155, 113834.
- Ottema, S., Mulet-Lazaro, R., Erpelinck-Verschueren, C., van Herk, S., Havermans, M., Arricibita Varea, A., ... Delwel, R. (2021). The leukemic oncogene EVI1 hijacks a MYC super-enhancer by CTCF-facilitated loops. *Nature Communications*, 12(1), 5679.
- Parola, M., & Pinzani, M. (2019). Liver fibrosis: Pathophysiology, pathogenetic targets and clinical issues. *Molecular Aspects of Medicine*, 65, 37–55.
- Qin, Y., Chen, F., Tang, Z., Ren, H., Wang, Q., Shen, N., ... Huang, L. (2022). Ligusticum chuanxiong Hort as a medicinal and edible plant foods: Antioxidant, anti-aging and neuroprotective properties in *Caenorhabditis elegans*. *Frontiers in Pharmacology*, 13, 1049890.
- Rai, U., Kosuru, R., Prakash, S., Singh, S. P., Birla, H., Tiwari, V., & Singh, S. (2019). Tetramethylpyrazine prevents diabetes by activating PI3K/Akt/GLUT-4 signalling in animal model of type-2 diabetes. *Life Sciences*, 236, 116836.
- Salgado-Albarran, M., Spath, J., Gonzalez-Barrios, R., Baumbach, J., & Soto-Reyes, E. (2022). CTCFL regulates the PI3K-Akt pathway and it is a target for personalized ovarian cancer therapy. *npj Systems Biology and Applications*, 8(1), 5.
- Wan, S. J., Ren, H. G., Jiang, J. M., Xu, G., Xu, Y., Chen, S. M., ... Xu, H. X. (2022). Two novel phenylpropanoid trimers from *Ligusticum chuanxiong* Hort with inhibitory activities on alpha-hemolysin secreted by staphylococcus aureus. *Frontiers in Chemistry*, 10, 877469.
- Wang, J., Wang, L., Zhou, H., Liang, X. D., Zhang, M. T., Tang, Y. X., ... Mao, J. L. (2022). The isolation, structural features and biological activities of polysaccharide from *Ligusticum chuanxiong*: A review. *Carbohydrate Polymers*, 285, 118971.
- Wang, M., Yao, M., Liu, J., Takagi, N., Yang, B., Zhang, M., ... Tian, F. (2020). *Ligusticum chuanxiong* exerts neuroprotection by promoting adult neurogenesis and inhibiting inflammation in the hippocampus of ME cerebral ischemia rats. *Journal of Ethnopharmacology*, 249, 112385.
- Wang, X. J., Xu, Y. H., Yang, G. C., Chen, H. X., & Zhang, P. (2015). Tetramethylpyrazine inhibits the proliferation of acute lymphocytic leukemia cell lines via decrease in GSK-3beta. *Oncology Reports*, 33(5), 2368–2374.
- Wu, H., Yang, T. Y., Li, Y., Ye, W. L., Liu, F., He, X. S., ... Li, J. M. (2020). Tumor necrosis factor receptor-associated factor 6 promotes hepatocarcinogenesis by interacting with histone deacetylase 3 to enhance c-Myc gene expression and protein stability. *Hepatology*, 71(1), 148–163.
- Wu, J. Z., Li, Y. J., Huang, G. R., Xu, B., Zhou, F., Liu, R. P., ... Li, X. J. (2021). Mechanisms exploration of *Angelica Sinensis Radix* and *Ligusticum chuanxiong* rhizoma herb-pair for liver fibrosis prevention based on network pharmacology and experimental pharmacology. *Chinese Journal of Natural Medicines*, 19(4), 241–254.
- Wu, M., Zhou, Y., Fei, C., Chen, T., Yin, X., Zhang, L., & Ren, Z. (2020). ID1 overexpression promotes HCC progression by amplifying the AURKA/MYC signaling pathway. *International Journal of Oncology*, 57(3), 845–857.
- Wu, X., Shu, L., Zhang, Z., Li, J., Zong, J., Cheong, L. Y., ... Hoo, R. L. C. (2021). Adipocyte fatty acid binding protein promotes the onset and progression of liver fibrosis via mediating the crosstalk between liver sinusoidal endothelial cells and hepatic stellate cells. *Advanced Science*, 8(11), e2003721.

Yang, J., & Xing, Z. (2021). Ligustilide counteracts carcinogenesis and hepatocellular carcinoma cell-evoked macrophage M2 polarization by regulating yes-associated protein-mediated interleukin-6 secretion. *Experimental Biology and Medicine*, 246(17), 1928–1937.

Zeng, X., Yuan, X., Cai, Q., Tang, C., & Gao, J. (2021). Circular RNA as an epigenetic regulator in chronic liver diseases. *Cells*, 10(8), 1945.

Zhang, H., Liu, C., Wang, M., & Sui, Y. (2020). Metabolic profiling of senkyunolide A and identification of its metabolites in hepatocytes by ultra-high-performance liquid chromatography combined with diode-array detector and high-resolution mass spectrometry. *Rapid Communications in Mass Spectrometry*, 34(21), e8894.